Surface & Coatings Technology 202 (2008) 5488–5492

Contents lists available at ScienceDirect

Surface & Coatings Technology

journal homepage: www.elsevier.com/locate/surfcoat

Effect of molybdenum and copper on S-phase layer thickness of low-temperature carburized austenitic stainless steel

M. Tsujikawa [a,*], M. Egawa [b], N. Ueda [b], A. Okamoto [b], T. Sone [b], K. Nakata [c]

[a] Department of Materials Science, Graduate School of Engineering, Osaka Prefecture University, 1-1 Gakuen-Cho Nakaku, Sakai, Osaka 599-8531, Japan
[b] Technology Research Institute of Osaka Prefecture, 2-7-1 Ayumino Izumi, Osaka 594-1157, Japan
[c] Joining and Welding Research Institute, Osaka University, 11-1 Mihogaoka Ibaraki, Osaka 567-0047, Japan

ARTICLE INFO

Available online 17 June 2008

Keywords:
S-phase
Austenitic stainless steel
Carburizing
Diffusion
Hardness
TEM

ABSTRACT

Surface hardening of austenitic stainless steels without degradation of corrosion resistance has been a subject of continuing interest in the field of surface engineering technology. This paper presents a method, using low-temperature plasma-carburized processing, to produce a hard and corrosion-resistant layer for austenitic stainless steels. The process is based on the diffusion of carbon and/or nitrogen from the surface into the austenitic substrate without forming any carbides or nitrides. The resultant carburized and/or nitrided surface layer shows highly superior saturation of carbon or nitrogen. It is called expanded austenite or S-phase. Important details of the S-phase have not been revealed yet, e.g., the formation of super saturated solid solution at constant processing temperature. For this study, austenitic stainless steel with 3 mass% copper was selected for use as a substrate of low-temperature carburizing. Actually, Cu shows no tendency for formation of carbides in steel. Samples were plasma-carburized using DC plasma apparatus under 667 Pa of mixed gas flow of 5% CH_4 + 45% H_2 + 50% Ar at 673 K or 723 K for various durations. The treated S-phase of steel with copper was compared to those of 304 steel and 316, 317 steels containing molybdenum. Results show that copper addition, just as molybdenum addition, similarly enhances carbon super saturation and the surface-layer hardness. Furthermore, the carburized layer depth was enhanced with copper addition as well as Mo addition. The effects of copper and molybdenum are discussed with measurements of the lattice constants in consideration of the size effect.

1. Introduction

Low-temperature nitriding hardens the surface layer of austenitic stainless steel and makes it nitride-free [1–6]. This surface layer, so-called S-phase, has hardness of ca. 1000 HV and retains the good corrosion resistance of austenitic stainless steel. This low-temperature diffusion processing is also effective for carburizing. Carburizing at temperatures lower than 400 °C hardens the surface of austenitic stainless steels and the corrosion-resistant layer without the use of carbides [7–14]. Essential information related to the S-phase has not been revealed yet. For example, a method for formation of a high hardness solid solution with a very high degree of super saturation is unclear. In practice, the request for a sufficiently thicker S-phase layer for heavy loaded sliding friction applications has further increased. However, it is difficult to increase the thickness because of the non-equilibrium microstructure produced by diffusion processing.

We reported the effect of molybdenum addition on increasing the layer thickness and hardness with increasing molybdenum content [7,8] using 304, 316, and 317 steels. The S-phase layer of the 316 steel is deeper than that of the 304 steel at the same plasma carburizing condition, which reflects the effect of molybdenum content. The surface hardness also increases with increasing Mo content. A larger-element material than Fe or Cr, such as Mo, extends the lattice. It is then easier for interstitial atoms to diffuse in the extended lattice. However, Mo is an element of easy formation of carbides. Does this affinity of Mo with carbon explain the easy diffusion and higher hardness? Is it only the size effect? The nature of the S-phase will reveal an effective means to control the layer characteristics.

In this study, the effect of alloy element on S-phase layer thickness for austenitic stainless steel is examined. The element selected for this study was copper. Copper has less affinity with carbon than either iron or chromium, but with larger ion size than either iron or chromium. The austenitic stainless steels used were 304 steel, 316 steel (2 mass% Mo), 317 steel (3 mass% Mo), and JIS SUS304-J3 steel (Fe-18 mass% Cr-8 mass%,Cr-3 mass% Cu). We elucidate the acceleration mechanism of carbon diffusion using molybdenum in comparison to that by copper.

2. Experimental procedure

Austenitic stainless steels used for this experiment were SUS304, SUS316, SUS317L, and SUS304-J3. All steels are specified in Japanese

* Corresponding author.
E-mail address: masatot@mac.com (M. Tsujikawa).

0257-8972/$ – see front matter © 2008 Elsevier B.V. All rights reserved.
doi:10.1016/j.surfcoat.2008.06.096

Table 1
Chemical compositions of austenitic stainless steel (mass%)

	C	Si	Mn	P	S	Ni	Cr	Mo	Cu
SUS304	0.060	0.40	0.94	0.037	0.003	8.3	18.8	0.21	0.31
SUS316	0.040	0.70	0.94	0.027	0.003	10.2	17.0	2.34	0.24
SUS317L	0.020	0.51	1.67	0.042	0.005	13.8	18.7	3.13	0.21
SUS304-J3	0.020	0.23	0.68	0.037	0.004	10.0	18.3	0.29	2.97

Table 2
Conditions for low-temperature plasma carburizing

Temperature (K)	673 or 723
Processing duration (ks)	7.2, 14.4, or 28.8
Gas flow (mL/s)	$5CH_4$–$45H_2$–50Ar
Total gas pressure (Pa)	6.67×10^2

Industrial Standard (JIS). The chemical compositions of the steels are presented in Table 1. These specimens were solution heat-treated for 2.7 ks at 1303 K. They were dry-ground slightly to the specimen shape of 25 mm width, 50 mm length, and 5 mm thickness and then mirror polished. These preparations rendered the specimens fully austenitic, as confirmed by X-ray diffraction (XRD) analysis.

Plasma carburizing was carried out using a DC plasma apparatus shown in Fig. 1. After each specimen was mounted on the cathode in a furnace and its vacuum-bell jar was evacuated to 1.33×10^{-1} Pa. The gas mixture of CH_4, H_2, and Ar was adjusted to 6.67×102 Pa. Then a DC glow-discharge was started. The specimens mounted on the cathode were heated by plasma bombardment and the carburizing temperature of the specimens was measured using a thermocouple. The plasma carburizing conditions are presented in Table 2. After the electrical discharge ended, the specimens were cooled to room temperature in vacuum.

The structures and compositions of the resultant carburized layers were characterized using various analytical techniques: metallographic analysis of cross-sections for layer morphology examination, thickness and hardness profile measurements, glow-discharge optical emission spectrometry (GDOES) for carbon distribution measurement, etc. The carbides were detected using XRD and transmission electron microscopy (TEM).

3. Results and discussion

3.1. Metallographic observations

Metallographic cross-sections of the surface layers of specimens carburized at 723 K are presented in Fig. 2. Aqua regia was used to reveal the alloyed layers' morphology. As the figure shows, the plasma-carburized surface layers were resistant to etching by the etchant used. No etched or corroded spots were observed in the surface layers.

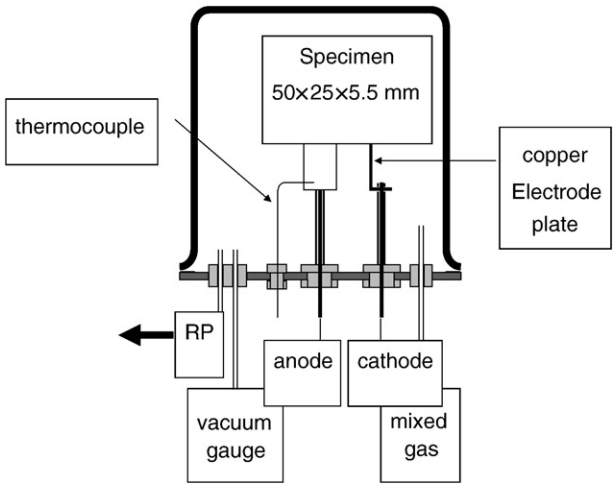

Fig. 1. Schematic feature of DC plasma apparatus.

Fig. 3 shows that the thickness of the carburized layer increased with increasing Mo or Cu content. The layer of 317L (3.13%-Mo) was thicker than those of the 304 steel specimens. Consequently, Mo was demonstrated to be an effective alloying element for thickening the surface layer by plasma carburization. The 304-J3 steel layer thickness is also greater than that of the 304 specimens. Results show that Cu is also effective as an additional element to thicken the carburized layer of austenitic stainless steel.

3.2. Hardness profiles

The cross-sectional hardness profile of each specimen surface was measured using a Knoop hardness tester under 0.1 N load. Fig. 4 depicts typical hardness profiles. Apparently, the surface-layer hardness decreases gradually from the surface to the core. Surface hardness is also increased by addition of Mo or Cu.

3.3. Carbon distribution

Fig. 5 shows typical carbon concentration profiles as analyzed by GDOES for plasma-carburized specimens. All carbon profiles on the different substrates display a similar pattern. Non-error functional type of diffusion occurred because the diffusion coefficient at higher carbon content in the super saturated region is expected to differ from that of the dilute region. Very high carbon content is obtained at the surface compared to that of the layer inside, which decreases quickly to a region of fair carbon content. The bottom half of the layer has carbon content that decreases gradually to the base level found in the substrate. Copper has a similar effect to that of molybdenum on the surface-layer thickness. The increase of the diffusion coefficient is readily apparent.

3.4. TEM microstructure

Fig. 6 portrays TEM observations and SAD patterns of the carburized layer of austenitic stainless steels with Mo or Cu. Electron diffraction patterns show FCC structures; there are no signs of crystalline carbides. Carbides were not detected using XRD analysis [15,16]. A high density of twins and dislocation was observed. It is probable that the formation of such a high density of crystal defects is one response of austenitic stainless steels to low-temperature plasma carburizing. These features are evidence of plastic deformation, and are induced by compressive residual stresses generated during plasma carburizing.

3.5. Lattice parameter

To examine whether the cause of the hardness rises and the diffusion coefficient increases, lattice constants of specimens before and after plasma processing were measured using XRD carried out with CuKα radiation. Fig. 7 presents changes in the lattice constant using additional elements before plasma processing. Molybdenum and copper are larger elements than either iron, chromium, or nickel. The lattice constant is therefore expanded linearly with increasing Mo content; it is increased with Cu addition. These samples were annealed to form a solid solution state of fully austenitic phase.

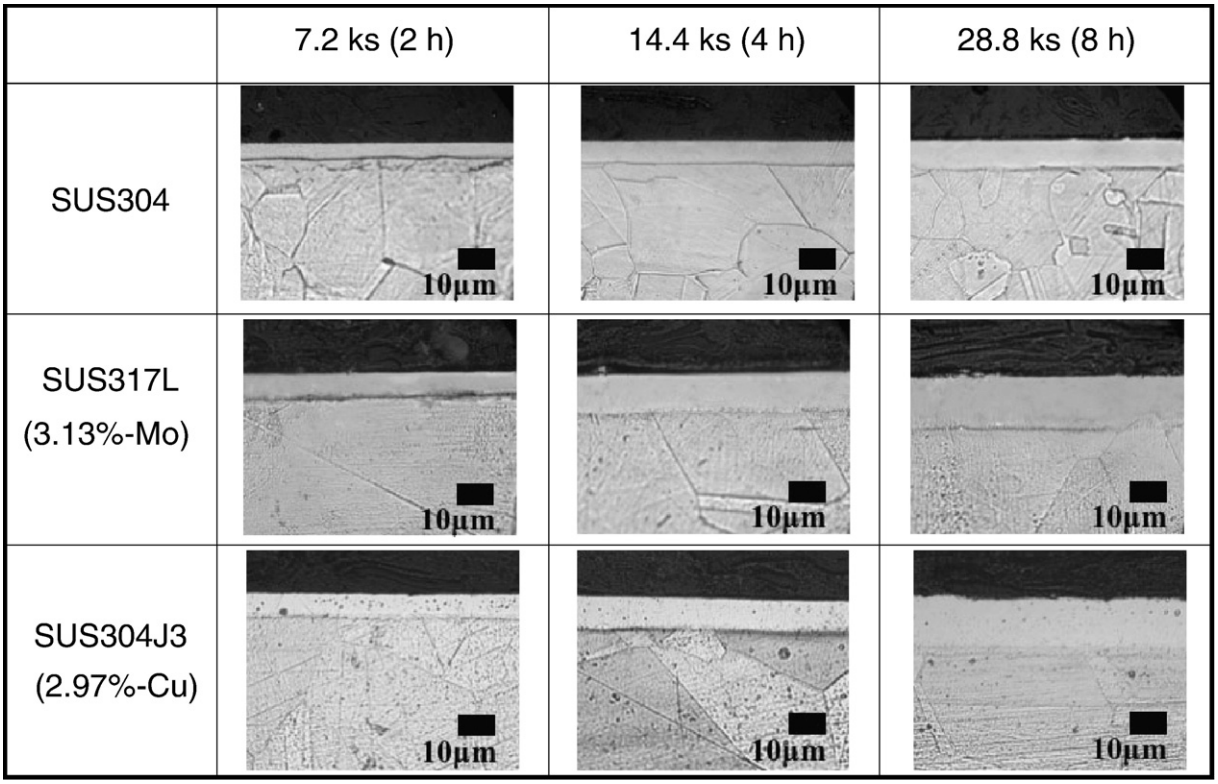

Fig. 2. Cross section views of specimens processed at 723 K.

The lattice constants of after-plasma-carburization specimens measured from the surface are shown in Fig. 8. The lattice constants of steels with different Mo content increase with increasing Mo contents. However, the increment is not linear relative to the Mo content. Higher Mo content expands the lattice to a greater degree than that predicted by a linear relation. This phenomenon is thought to be the influence of lattice expansion effects by an interstitial solution of carbon. The more that super saturation occurs, the more the lattice expands. The effect of Mo or Cu addition is multiplied with this effect of carbon.

Reportedly, addition of molybdenum to steel attracts interstitial atoms, according to Wada [17] and Murayama [18]. The reason for this is inferred to be the affinity of molybdenum to nitrogen or carbon.

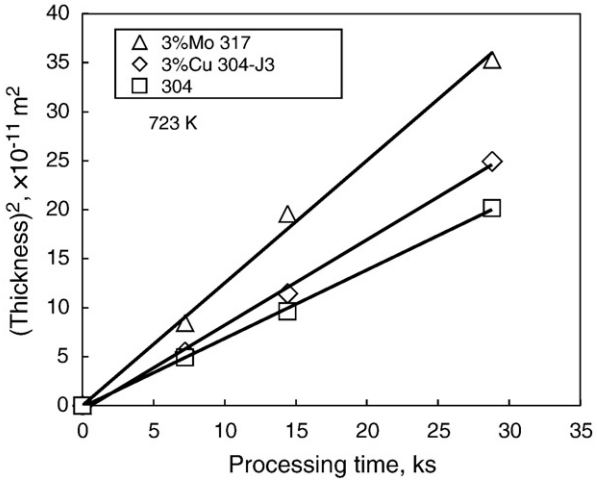

Fig. 3. Surface-layer thickness of the specimens.

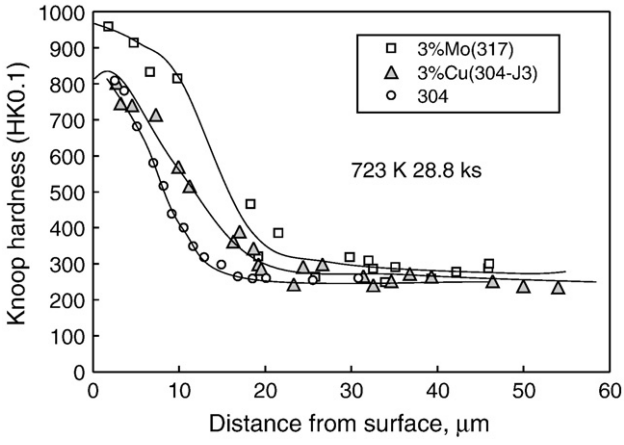

Fig. 4. Depth profile of Knoop hardness (723 K×28.8 ks).

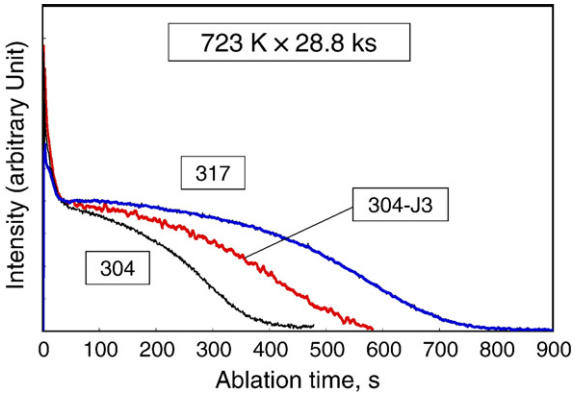

Fig. 5. GDOES depth profile of carbon of carburized samples.

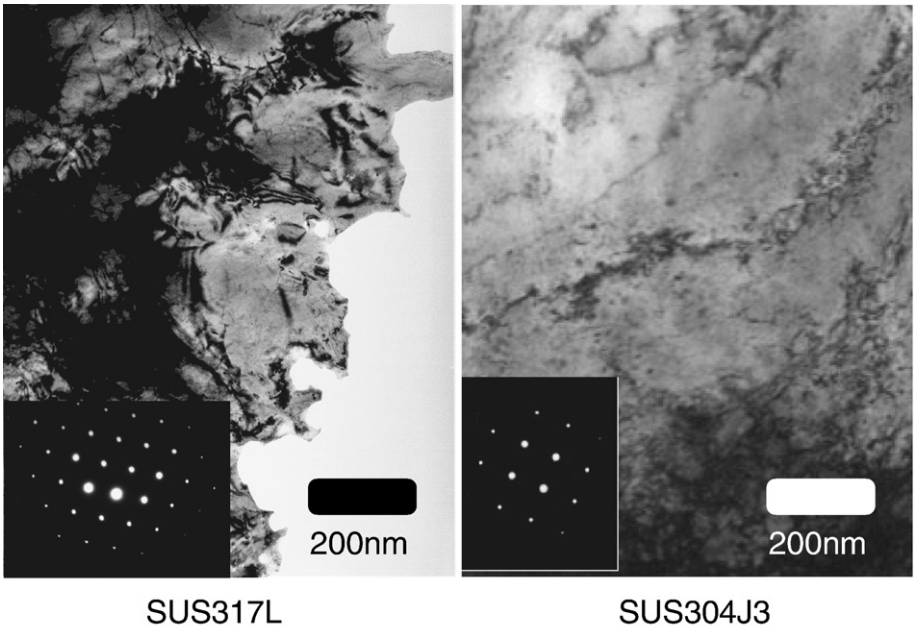

Fig. 6. TEM micrographs of carburized samples under 723 K, 28.8 ks.

Another reason is the lattice expansion effect by the large substitutional alloying element. The relationship between the lattice constant of substrate and the hardness and layer thickness of processed samples is presented in Fig. 9. The addition of copper, which is an element showing no tendency to form carbide in steel, displays a similar tendency to that of molybdenum for increasing hardness and layer thickness. The result suggests that, because of the lattice expansion effect, the hardness increases and layer thickness increases with Mo or Cu addition.

4. Conclusions

Surface hardness and thickness of a carburized layer of austenitic stainless steel treated using low-temperature plasma carburizing can be improved by addition of molybdenum or copper, and the hardness and layer thickness increased with increasing their content. There was no evidence of carbides in the hard surface layer of copper addition steel and molybdenum addition steel, observed by TEM. The treated surface hardness and layer thickness increased linearly with the lattice constant of the substrate, regardless of the added element. These results suggest that the enhancement of carbon super saturation by Mo or Cu addition is caused by the lattice expansion effect of the large elements. The same effect could be true, that is, the lattice expansion by supersaturated carbon induces the further solution of carbon.

References

[1] K. Ichii, K. Fujimura, T. Takase, Netsu Shori 25 (1985) 191.
[2] Z.L. Zhang, T. Bell, Surf. Eng. 1 (1985) 131.
[3] A. Nishimoto, K. Ichii, K. Nakao, M. Takai, K. Akamatsu, Stainless Steel 2000, Maney Publishing, 2000, p. 289.
[4] N. Yamauchi, N. Ueda, K. Demizu, A. Okamoto, T. Sone, K. Oku, T. Kouda, K. Ichii, K. Akamatsu, Proc. Int. Semi. on Thermochem. Surf. Engi. Stainless Steel, 2001, p. 247.
[5] D.L. Williamson, P.J. Wilbur, F.R. Fickett, S. Parascandala, Proc. Int. Semi. on Thermochem. Surf. Engi. Stainless Steel, 2001, p. 332.

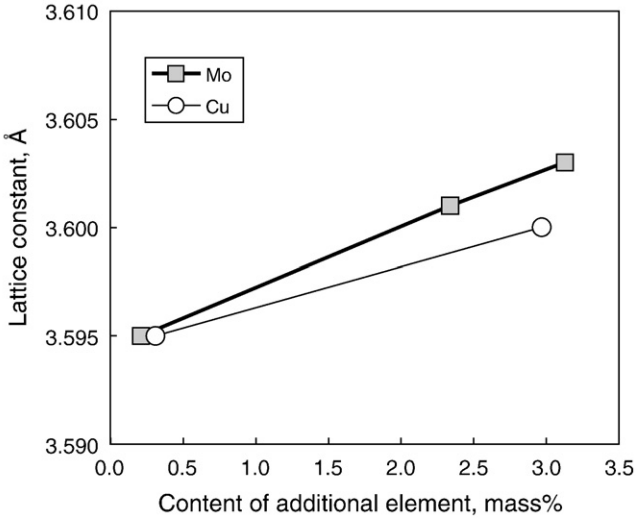

Fig. 7. Lattice constants of samples before processing.

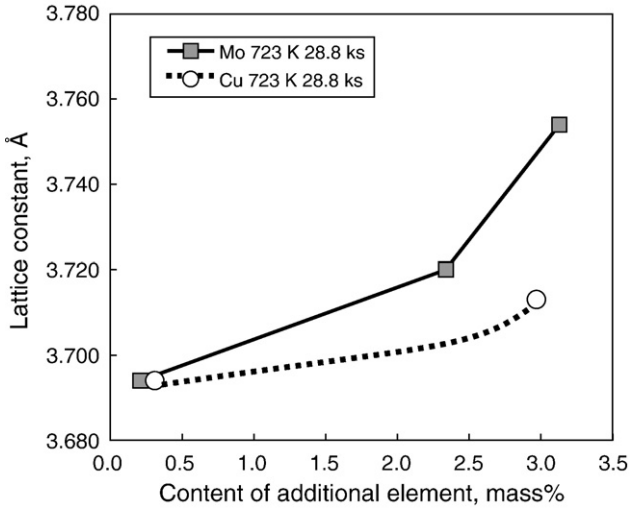

Fig. 8. Lattice constants of samples after processing.

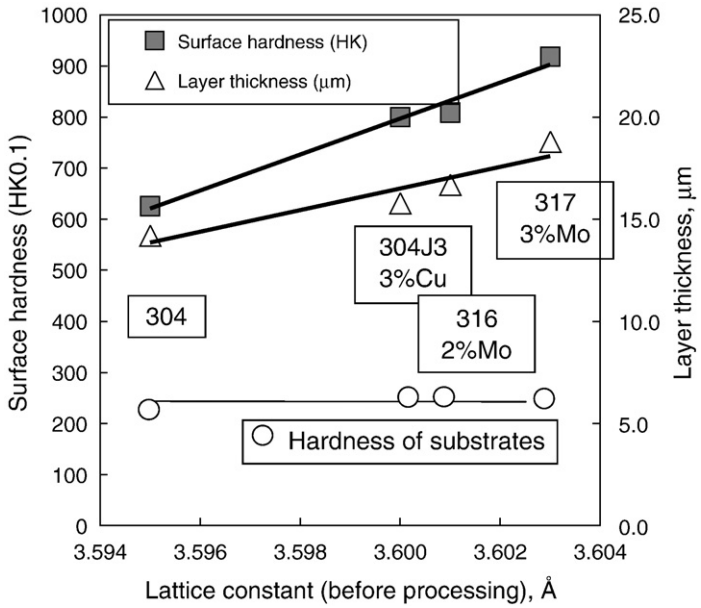

Fig. 9. Relationship between lattice constant and properties.

[6] M. Tsujikawa, N. Yamauchi, N. Ueda, T. Sone, Surf. Coat. Technol. 200 (1–4) (2005) 507.
[7] M. Tsujikawa, D. Yoshida, N. Yamauchi, N. Ueda, T. Sone, Mater. Trans. 46 (2005) 863.
[8] M. Tsujikawa, N. Yamauchi, N. Ueda, T. Sone, Y. Hirose, Surf. Coat. Technol. 193 (1–3) (2004) 309.
[9] Z.L. Zhang, T. Bell, Proc. Int. Semi. on Thermochem. Surf. Engi. Stainless Steel, 2001, p. 1.
[10] Y. Sun, X. Li, T. Bell, Proc. Int. Semi. on Thermochem. Surf. Engi. Stainless Steel, 2001, p. 51.
[11] T. Bell, Y. Sun, Proc. Int. Semi. on Thermochem. Surf. Engi. Stainless Steel, 2001, p. 275.
[12] Y. Sun, X.Y. Li, T. Bell, Surf. Eng. (1999) 49.
[13] Y. Sun, X.Y. Li, T. Bell, Mater. Sci. Tech. 15 (1999) 1171.
[14] Y. Sun, J. Mater. Process. Technol. 168 (2005) 189.
[15] M. Tsujikawa, S. Noguchi, N. Ueda, N. Yamauchi, T. Sone, Surf. Coat. Technol. 201 (9–11) (2007) 5102–5107.
[16] M. Tsujikawa, S. Noguchi, N. Yamauchi, N. Ueda, A. Okamoto, T. Sone, Plasma Processes Polym. 4 (2007) S752–S756.
[17] M. Wada, K. Hosoi, O. Nishikawa, Acta Metal. 30 (1982) 1005.
[18] M. Murayama, K. Hono, H. Hirukawa, T. Ohmura, S. Matsuoka, Scr. Mater. (1999) 467.